Traversa et al. SUPPLEMENTARY MATERIAL

SUPPLEMENTARY MATERIALS AND METHODS

Rice growth and floral induction

Plants of *Oryza sativa* cv. Nipponbare were grown under LD conditions for 6 weeks in a growth chamber under a 14.5-hour photoperiod. Batches of plants were shifted to SD conditions (10-hour photoperiod) at time point 0 (i.e., after 6 weeks), and after 4, 8, and 13 days. This design enabled us to collect shoot apices simultaneously from plants that had been under SD conditions for varying durations (0, 5, 9, and 13 days). Harvesting began on the 13th day, starting from Zeitgeber 0 (the moment the lights were switched on). Meristems were hand-dissected under a stereomicroscope. Eight distinct biological replicates were collected and pooled at every time point, and the collection process of the different time points was randomized.

Nuclei isolation and sorting

Freshly collected shoots were kept on ice and immediately processed for nuclear extraction. Nuclei isolation was performed as described in (Lu et al. 2017) with few modifications. SAMs were homogenized in ice cold 1.5 ml Nuclei Isolation Buffer (NIB; 15 mM Tris-HCl pH = 7.5, 20 mM NaCl, 80 mM KCl, 0.5 mM Spermine, 5 mM 2-Mercaptoethanol, 0.2% Triton X-100) with a handheld homogenizer (T10 basic ULTRA-TURRAX, IKA, China, Guangzhou): for every sample, 5 pulses at medium power were used. Homogenates were then filtered two times in Miracloth (Millipore, Merck, Germany, Darmstadt), layered on the top of 1.5 ml of Dense Sucrose Buffer (DSB; 20 mM Tris-HCl pH=8, 2 mM $MgCl_2$, 2 mM EDTA, 15 mM 2-Mercaotoethanol, 1.7 M Sucrose, 0.2% Triton X-100) and centrifuged at 3000g for 30 min in a swinging-bucket centrifuge pre-chilled at 4°C. Next, the nuclei-enriched pellet was resuspended in 500 µL NIB and filtered in a 30 µm cell strainer (CellTrics, Sysmex, Japan, Kobe) before sorting. Crude nuclei were stained with 4,6-Diamidino-2-phenylindole (DAPI) and loaded into a flow cytometer (FACSAria II, BD Bioscienses, Franklin Lake, New Jersey, USA). The gating strategy used for nuclei sorting is summarized in Fig. S14. In short, nuclei were separated from debris and background noise by setting a gate in the DAPI fluorescence channel. The typical multiple peaks (corresponding to the different DNA ploidy) area was selected on the SSC/DAPI plot as the population to be sorted, checked for consistency on the

DAPI mean fluorescence intensity (MFI) histogram and compared to a no DAPI stained control do check for impurities. As for FACS settings, the flow rate was constantly adjusted to achieve no more than 1000 events/s and a 70 µm nozzle was used. A total of 7000 nuclei were sorted based on their size and strength of DAPI signal and collected in 300 µL of Nuclei Resuspension Buffer (NRB; 1.8 mM KH2PO4, 10 mM NaH2PO4, KCl 2.7 mM, 137 mM NaCl, 0.2 U/µL RNAse inhibitor (New England Biolabs, Ipswich, United Kingdom), 1% bovine serum albumin (BSA)).

Sequencing

Single nuclei libraries were prepared using the 10x Chromium single cell gene expression workflow RNAseq v3.1, double index. Illumina paired-end library had the following structure: P5 and P7 (for the Illumina bridge amplification), two sequencing primers annealing region, 16bp 10x barcode for the cell identification, 12bp UMI to count the transcripts, cDNA from the 3' UTR region of the gene and the sample index to demultiplex the pool of samples loaded on the sequencer. Amplified libraries were checked on a bioanalyzer 2100 and quantified with picogreen reagent. Libraries with distinct indexes were multiplexed and after cluster generation on Flow Cell they were sequenced for 28-10-10-90 bases in the paired-end mode on a Novaseq 6000 sequencer.

BIOINFORMATICS ANALYSIS

Pre-processing and computation of count matrices

Unique molecular identifiers and cell barcoded were extracted from raw FASTQ files by UMI-tools extract (Smith et al. 2017). Reads were aligned to the *IRGSP-1.0* assembly of the *Oryza sativa ssp. japonica cv.* Nipponbare genome as available from RAPDB (Sakai et al. 2013) (2004-01 update), by using the STAR aligner (Dobin et al. 2013). Alignments in bam format were processed by UMI-tools dedup to remove duplicate molecules. Summarization of reads counts with respect to reference genome annotation was performed by Featurecounts (Liao et al. 2014).

Quality control and clustering

Gene counts matrices were loaded in Seurat V 5.1.0 (Satija et al. 2015). Data was processed following publicly available code and tutorials (https://satijalab.org/seurat/articles/pbmc3k_tutorial.html). Nuclei having < 200 genes with a

count >=1, and cells with >10% reads in organellar genes were discarded. Cell cycle genes were inferred by cross-referencing the complete collection of *A.thaliana* cell cycle genes as reported by Vandepoele et al (Vandepoele et al. 2002) with orthologs in *O. sativa* as according to Plaza V5 (Van Bel et al. 2022). These genes were removed from further computations. Normalization, scaling, and variable feature selection was performed using the vst transformation with 4000 features. Clusters were inferred using Seurat's SNN-graph approach with a resolution of 0.4 and considering the first 20 principal components. Markers genes were identified by using the Seurat FindAllMarkers() function with the following parameters: only.pos = FALSE, min.pct = 0.1, logfc.threshold = 0.25.

Pseudo-time and functional enrichment analyses

Pseudo-time analysis was performed by applying Monocle3 (Trapnell et al. 2014) as provisioned in the scPlant (Cao et al. 2023) package Developmental trajectories were inferred using the learn_graph() function, and initial time points were manually annotated by superimposing the experimental design (time TP1) to the UMAP plot. Gene modules were determined by using the find_gene_modules() function in Monocle 3, with a resolution of 1e-3. The graph_test() utility was applied to identify differentially expressed genes at different pseudotime modules. A q-value threshold of 0.05 for statistical significance was applied.

Functional enrichment analyses were performed by running RunGSEA_plant() function from scPlant on the complete collection of cluster marker genes identified by Seurat. Topic modeling on GSEA results was performed by a latent discriminant analysis as implemented by the runLDA() function in scPlant. The value of k (number of topics) was arbitrarily set to 6.

Bulk RNAseq analysis

Reads from Gòmez-Ariza (Gómez-Ariza et al. 2019) et. al. were downloaded from https://www.ncbi.nlm.nih.gov/geo/query/acc.cgi?acc=GSE90493 and aligned to the *IRGSP-1.0* assembly of the *Oryza sativa ssp. japonica cv. Nipponbare* genome by means of the STAR (Dobin et al. 2013) software. Gene expression levels, with respect to the reference annotation of the IRGSP-1.0 assembly, were estimated by RSEM (Li et al. 2011). Differential analyses of gene expression were executed by means of the edgeR (Robinson et al. 2010); the Genewise Negative Binomial Generalized (glmQLFTest) was applied to test for statistically significant differences. P-values were corrected using the Benjamini Hochberg procedure for the control of the false

discovery rate. Only genes showing a P-value ≤ 0.05 following the FDR adjustment were considered differentially expressed (DEGs).

Expression profile of genes associated with SAM/inflorescence identity

A collection of manually curated markers associated with SAM/inflorescence identity was compiled from the literature and from the bulk-RNA sequencing analysis (Supplementary Table 5). Two independent lists were evaluated: the first contains well characterized genes whose expression in SAM tissues had been already dissected by detailed expression profiling (i.e. *in situ* hybridization). The second list contains genes differentially expressed and up-regulated (log_2(FC) > 0 and FDR ≤ 0.05) from bulk-RNA sequencing analysis performed by Mineri et. Al. at the SAM during floral induction after 12 days of SD exposure (Mineri et al. 2023)

Pseudo-bulk RNA-seq dataset

The expression profiles from snRNA sequencing were aggregated *in-silico* by time point in a pseudo-bulk-RNAseq dataset and compared with the corresponding time point from bulk RNA sequencing (Gómez-Ariza et al. 2019), both expressed as logarithmic transformed counts per million (log_2(CPM+0.5)). To derive the pseudo-bulk RNA-seq dataset, read counts from snRNA-seq were summed per gene per time point. Subsequently, CPM were calculated for both bulk and pseudo-bulk data to allow comparisons between the two datasets.

Statistical inference

Correlation coefficients were calculated through the cor.test() function available from the basic R set of functions (R code team, 2022).
The same collection of functions was used to compare our clusters-specific genes and those from Zong et Al. through a hypergeometric test performed with the function phyper().

Promoter analysis

The complete collection of plant transcription factors binding sites (TFBS), according to the Jaspar (Rauluseviciute et al. 2024) database was retrieved from: https://jaspar2020.genereg.net/search?q=&collection=CORE&tax_group=plants.

TFBS enrichment in Seurat's clusters marker genes, Monocle 3's pseudotime modules marker genes, and genes differentially expressed between different time points in the Gómez-Ariza

et Al. (Gómez-Ariza et al. 2019) bulk RNA-seq dataset was computed by pscan (Zambelli et al. 2009). A p-value threshold of 0.05 was applied to delineate statistical significance.

Similarity of TFBS enrichment profiles between gene sets was quantified by computing the Pearson correlation coefficient of pscan p-values. Modules, clusters and time points were gathered into groups manually, based on the heatmap of correlation coefficients shown in figure 1C.

TFBS profiles were aggregated in families/classes of transcription factors (TF) according to the annotation from Jaspar database available at https://jaspar.elixir.no/ and the total number of enriched TFBS associated with every family, in every group was counted. A TF family was considered enriched if TFBS assigned to that family were overrepresented in that group, compared to the other groups according to a Fisher's exact test (p-value threshold 0.05) . The ternary plot was obtained using the TernaryPlot() function from the Ternary package https://zenodo.org/records/12825289 downloadable on the R programming language.

SUPPLEMENTARY METHODS REFERENCES

Cao S, He Z, Chen R, et al (2023) scPlant: A versatile framework for single-cell transcriptomic data analysis in plants. Plant Commun 4:. https://doi.org/10.1016/j.xplc.2023.100631

Dobin A, Davis CA, Schlesinger F, et al (2013) STAR: Ultrafast universal RNA-seq aligner. Bioinformatics 29:. https://doi.org/10.1093/bioinformatics/bts635

Gómez-Ariza, J., Brambilla, V., Vicentini, G. et al. A transcription factor coordinating internode elongation and photoperiodic signals in rice. Nat. Plants 5, 358–362 (2019). https://doi.org/10.1038/s41477-019-0401-4

Li, B., Dewey, C.N. RSEM: accurate transcript quantification from RNA-Seq data with or without a reference genome. *BMC Bioinformatics* 12, 323 (2011). https://doi.org/10.1186/1471-2105-12-323

Liao Y, Smyth GK, Shi W (2014) FeatureCounts: An efficient general purpose program for assigning sequence reads to genomic features. Bioinformatics 30:. https://doi.org/10.1093/bioinformatics/btt656

Lu Z, Hofmeister BT, Vollmers C, et al (2017) Combining ATAC-seq with nuclei sorting for discovery of cis-regulatory regions in plant genomes. Nucleic Acids Res 45:. https://doi.org/10.1093/nar/gkw1179

Mineri L, Cerise M, Giaume F, et al (2023) Rice florigens control a common set of genes at the shoot apical meristem including the F-BOX BROADER TILLER ANGLE 1 that regulates tiller angle and spikelet development. Plant Journal 115:1647–1660. https://doi.org/10.1111/tpj.16345

R Core Team (2022). R: A language and environment for statistical computing. R Foundation for Statistical Computing, Vienna, Austria. URL https://www.R-project.org/

Rauluseviciute I, Riudavets-Puig R, Blanc-Mathieu R, Castro-Mondragon JA, Ferenc K, Kumar V, Lemma RB, Lucas J, Chèneby J, Baranasic D, Khan A, Fornes O, Gundersen S, Johansen M, Hovig E, Lenhard B, Sandelin A, Wasserman WW, Parcy F, Mathelier A JASPAR 2024: 20th anniversary of the open-access database of transcription factor binding profiles *Nucleic Acids Res.* in_press; doi: 10.1093/nar/gkad1059

Robinson MD, McCarthy DJ, Smyth GK. edgeR: a Bioconductor package for differential expression analysis of digital gene expression data. Bioinformatics. 2010 Jan 1;26(1):139-40. doi: 10.1093/bioinformatics/btp616. Epub 2009 Nov 11. PMID: 19910308; PMCID: PMC2796818.

Sakai H, Lee SS, Tanaka T, et al (2013) Rice annotation project database (RAP-DB): An integrative and interactive database for rice genomics. Plant Cell Physiol 54:. https://doi.org/10.1093/pcp/pcs183

Satija R, Farrell JA, Gennert D, et al (2015) Spatial reconstruction of single-cell gene expression data. Nat Biotechnol 33:. https://doi.org/10.1038/nbt.3192

Smith T, Heger A, Sudbery I (2017) UMI-tools: Modeling sequencing errors in Unique Molecular Identifiers to improve quantification accuracy. Genome Res 27:. https://doi.org/10.1101/gr.209601.116

Trapnell C, Cacchiarelli D, Grimsby J, Pokharel P, Li S, Morse M, Lennon NJ, Livak KJ, Mikkelsen TS, Rinn JL. The dynamics and regulators of cell fate decisions are revealed by pseudotemporal ordering of single cells. Nat Biotechnol. 2014 Apr;32(4):381-386. doi: 10.1038/nbt.2859. Epub 2014 Mar 23. PMID: 24658644; PMCID: PMC4122333.

Van Bel M, Silvestri F, Weitz EM, et al (2022) PLAZA 5.0: Extending the scope and power of comparative and functional genomics in plants. Nucleic Acids Res 50:. https://doi.org/10.1093/nar/gkab1024

Vandepoele K, Raes J, De Veylder L, et al (2002) Genome-wide analysis of core cell cycle genes in Arabidopsis. Plant Cell 14:. https://doi.org/10.1105/tpc.010445

Zambelli F, Pesole G, Pavesi G (2009) Pscan: Finding over-represented transcription factor binding site motifs in sequences from co-regulated or co-expressed genes. Nucleic Acids Res 37:. https://doi.org/10.1093/nar/gkp464

Zong J, Wang L, Zhu L, et al (2022) A rice single cell transcriptomic atlas defines the developmental trajectories of rice floret and inflorescence meristems. New Phytologist 234:. https://doi.org/10.1111/nph.18008

SUPPLEMENTARY FIGURES

- Fig. S1 Distribution of reads count per nuclei
- Fig. S2 Distribution of the number of transcripts per nuclei
- Fig. S3 – UMAP of clusters;
- Fig. S4 – Proportion of nuclei in each cluster associated to each time point;
- Fig. S5 – Semantic clustering analysis;
- Fig. S6 – Pseudo time trajectories;
- Fig. S7 – Correspondence clusters and modules;
- Fig. S8 – Expression of modules specific genes;
- Fig. S9A – Expression of SAM genes from in situ experiments across clusters;;
- Fig. S9B - Expression of SAM genes differentially expressed and up-regulated from bulk-RNAseq experiments by Mineri et Al. across clusters;
- Fig. S10A – Proportion of nuclei expressing SAM genes from in situ experiments per time point;
- Fig. S10B – Proportion of nuclei expressing SAM genes differentially expressed and up-regulated from bulk-RNAseq experiments by Mineri et Al. per time point;
- Fig. S11A – Correlation of common genes between pseudo-bulk-RNAseq and bulk-RNAseq from Gómez-Ariza et Al. across the different time points;
- Fig. S11B - Correlation of genes between pseudo-bulk-RNAseq and bulk-RNAseq from Gómez-Ariza et Al. at different expression levels across the different time points;
- Fig. S12 – Correlation of SAM genes from supplementary Table S5 across the different time points;
- Fig. S13 – Proportion of shared genes between our clusters with those from Zong et. al.;
- Fig. S14 - Fluorescence-activated sorting of nuclei.

SUPPLEMENTARY TABLES

- Supplementary Table S1 – Raw reads quality metrics;

- Supplementary Table S2 –Number of features and cluster assigned per nuclei;
- Supplementary Table S3 – Cluster-specific genes;
- Supplementary Table S4 – Module-specific genes;
- Supplementary Table S5 – SAM associated genes from in situ experiments and/or differentially expressed and up-regulated from Mineri et Al.;
- Supplementary Table S6 - TF genes with a significant variation of the expression across the four time points from the pseudo-bulk-RNAseq

FIG. S1

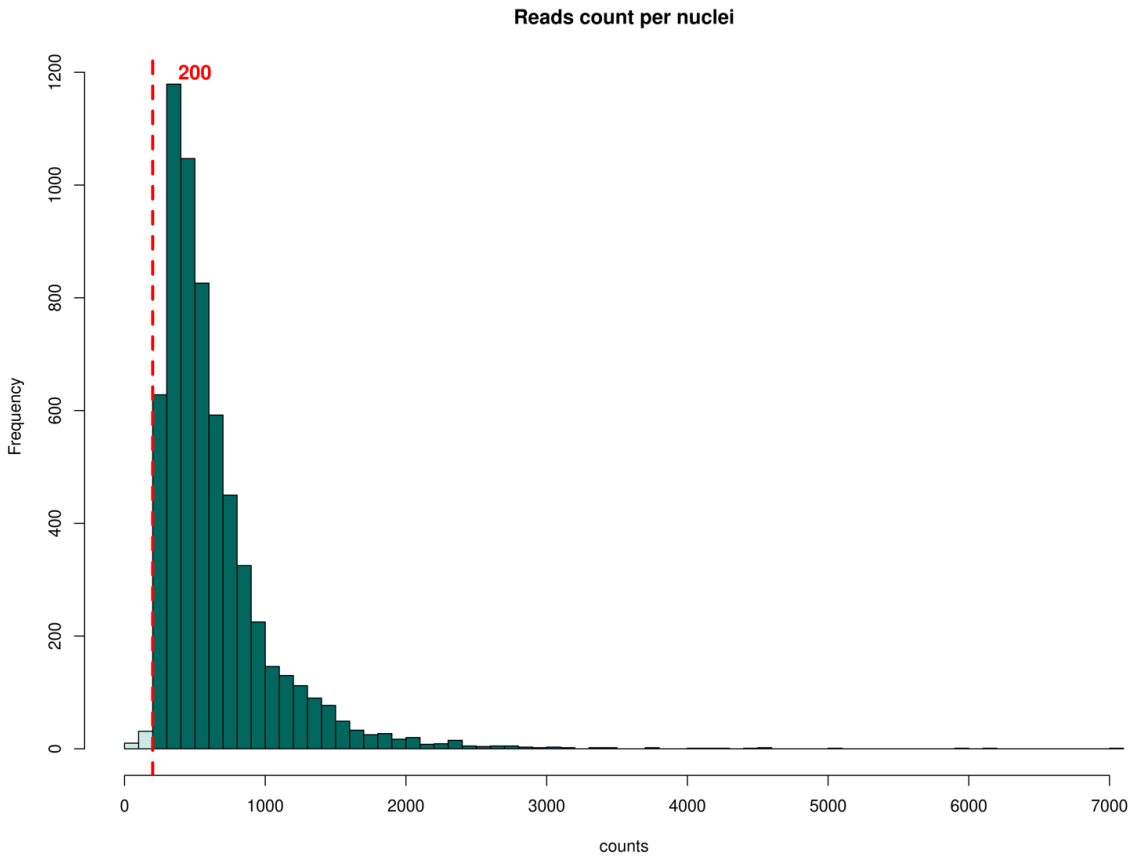

FIG. S2

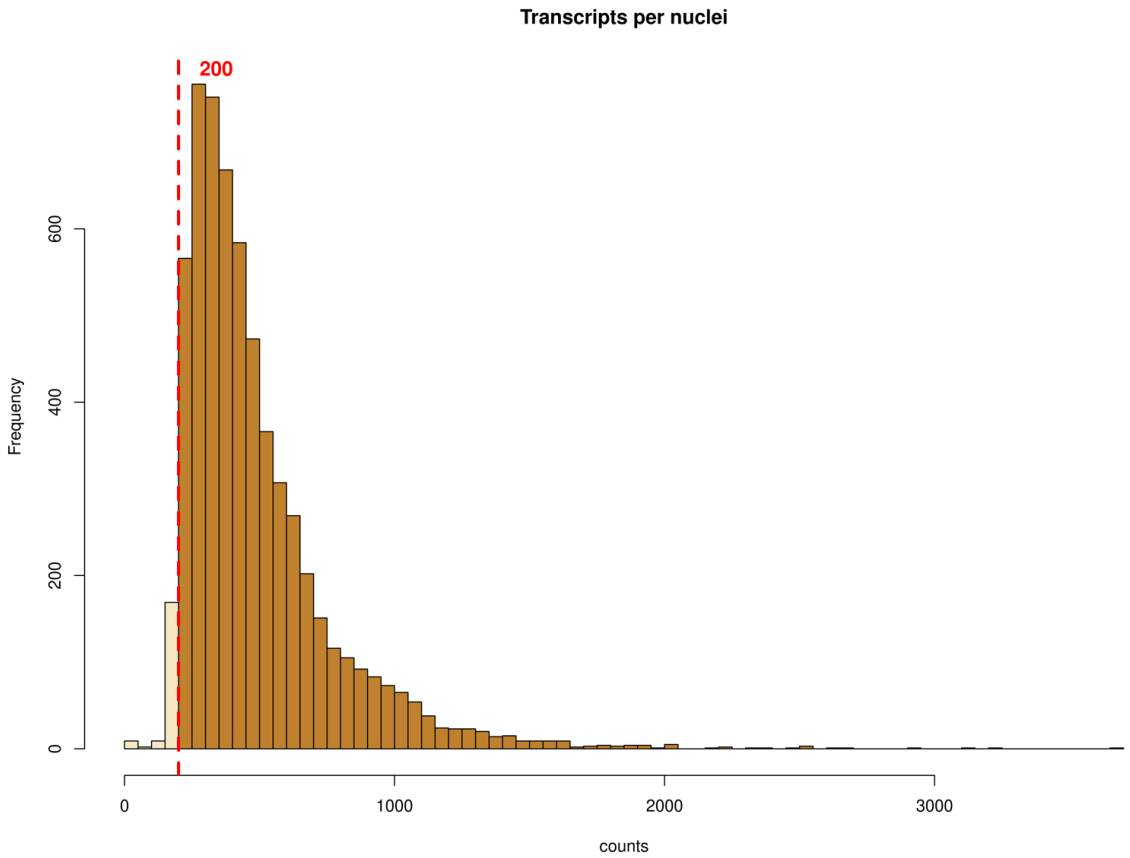
Transcripts per nuclei
200
Frequency
0
200
400
600
0
1000
2000
3000
counts

FIG. S3

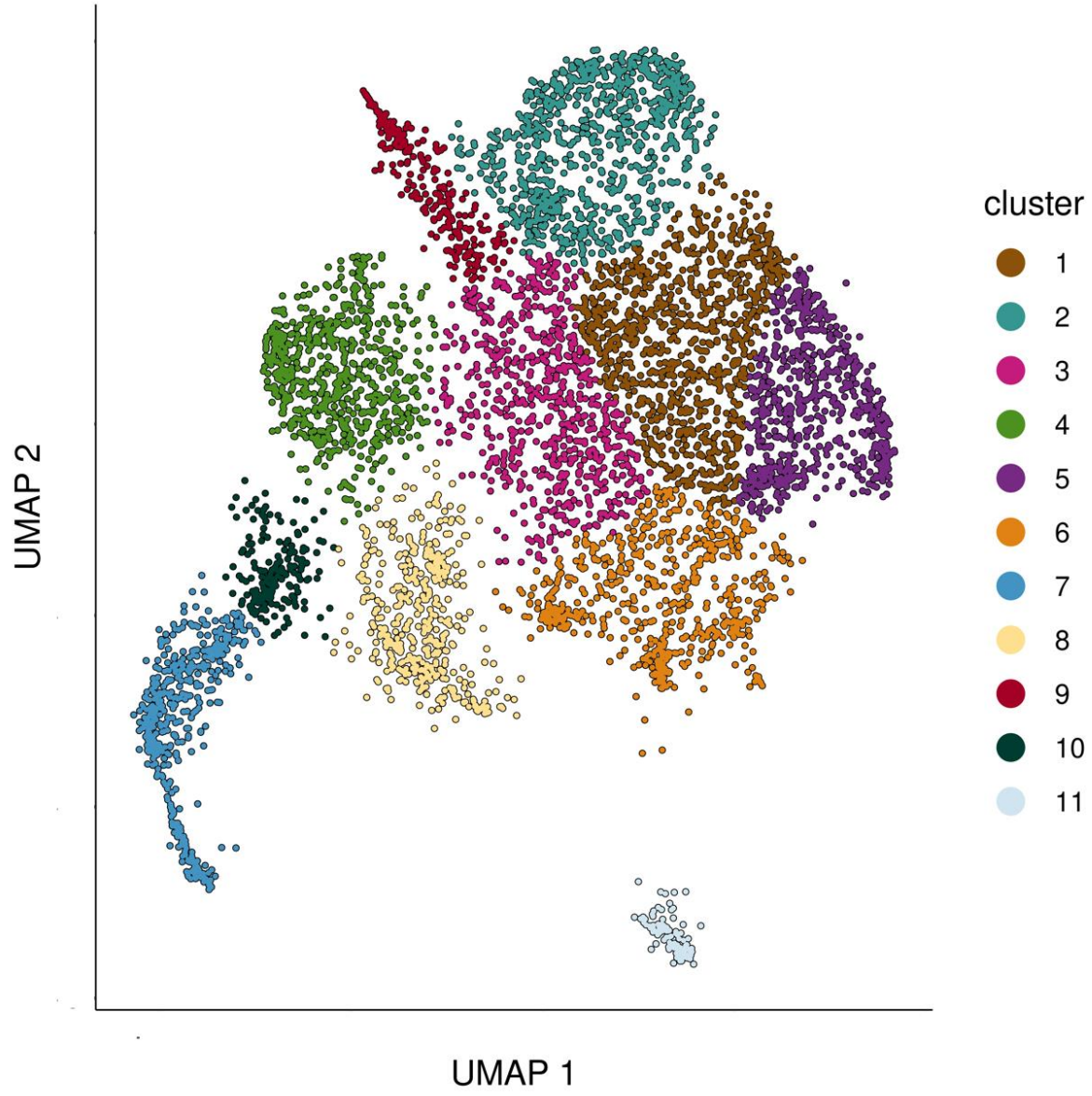

FIG. S4

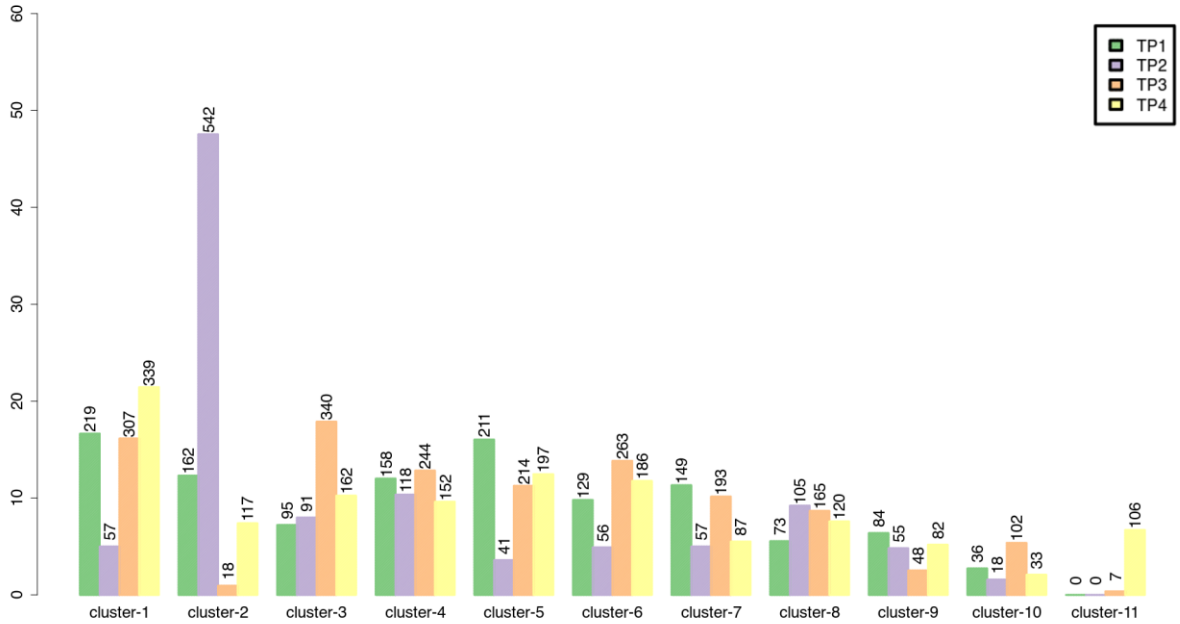
TP1
TP2
TP3
TP4
0
10
20
30
40
50
60
219
57
307
339
162
542
18
117
95
91
340
162
158
118
244
152
211
41
214
197
129
56
263
186
149
57
193
87
73
105
165
120
84
55
48
82
36
18
102
33
0
0
7
106
cluster-1
cluster-2
cluster-3
cluster-4
cluster-5
cluster-6
cluster-7
cluster-8
cluster-9
cluster-10
cluster-11

FIG. S5

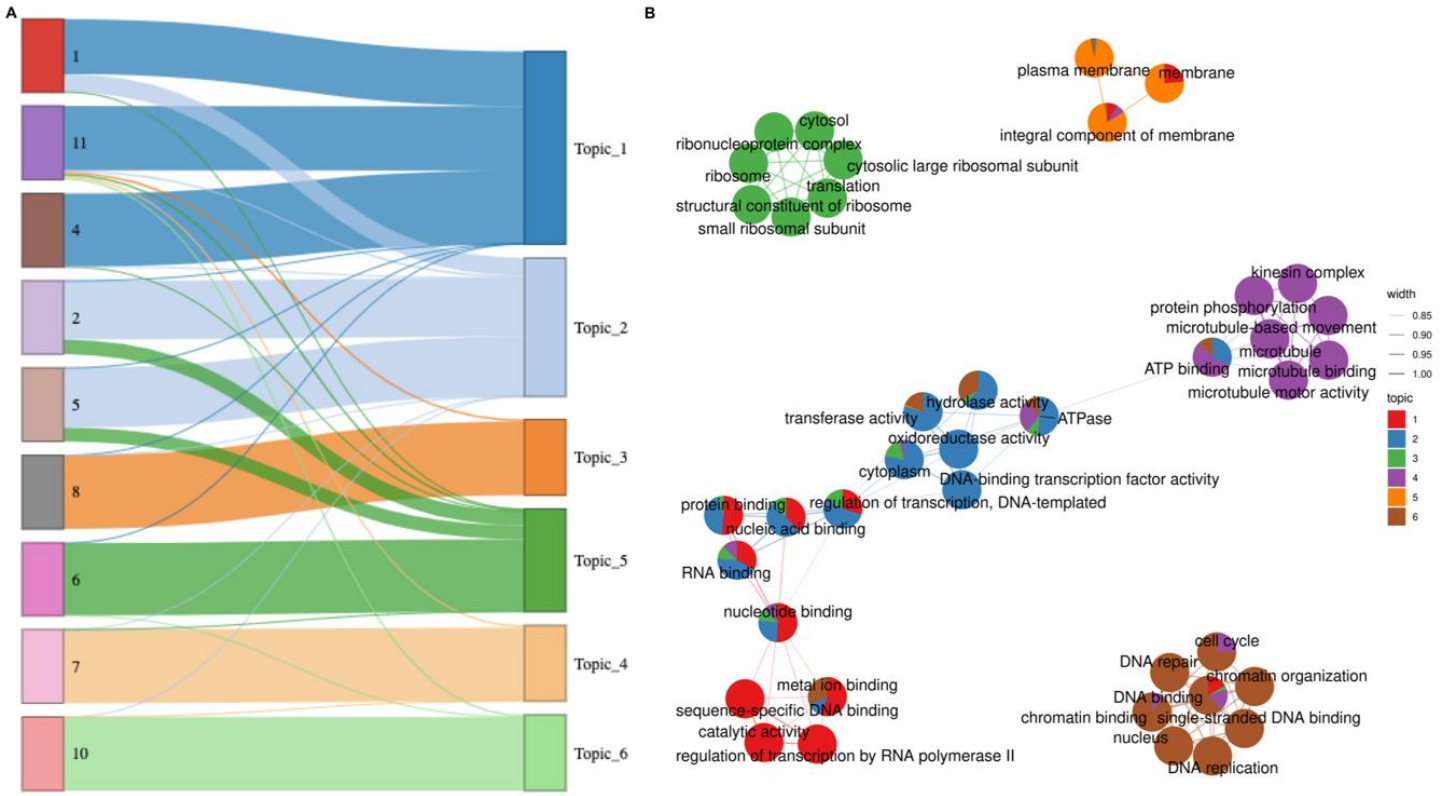
A
1
11
4
2
5
8
6
7
10
Topic_1
Topic_2
Topic_3
Topic_5
Topic_4
Topic_6
B
plasma membrane
membrane
integral component of membrane
cytosol
ribonucleoprotein complex
ribosome
translation
structural constituent of ribosome
small ribosomal subunit
cytosolic large ribosomal subunit
kinesin complex
protein phosphorylation
microtubule-based movement
microtubule
ATP binding
microtubule binding
microtubule motor activity
hydrolase activity
transferase activity
ATPase
oxidoreductase activity
cytoplasm
DNA-binding transcription factor activity
protein binding
regulation of transcription, DNA-templated
nucleic acid binding
RNA binding
nucleotide binding
metal ion binding
sequence-specific DNA binding
catalytic activity
regulation of transcription by RNA polymerase II
cell cycle
DNA repair
chromatin organization
DNA binding
chromatin binding
single-stranded DNA binding
nucleus
DNA replication
width
0.85
0.90
0.95
1.00
topic
1
2
3
4
5
6

FIG. S6

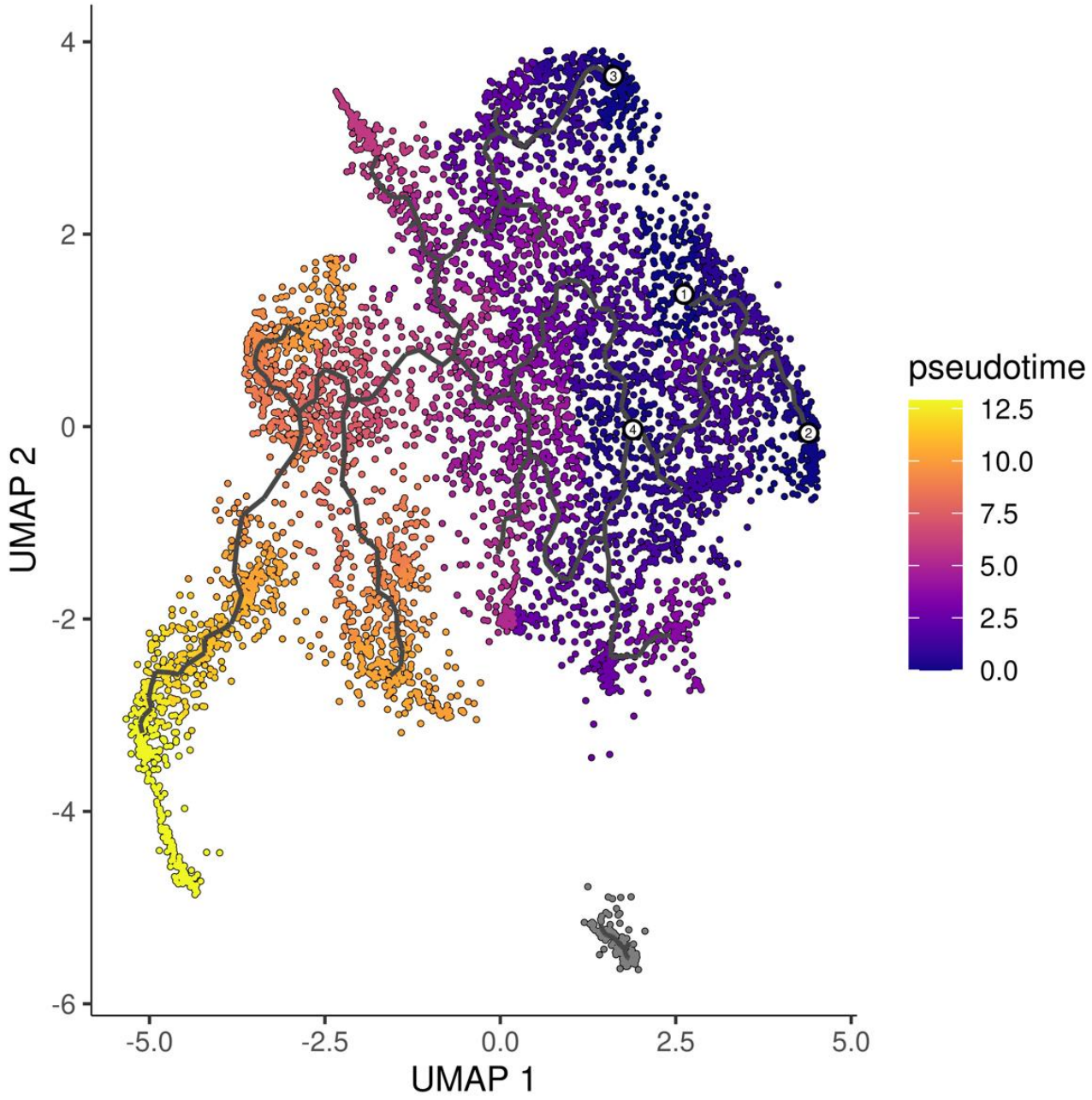
UMAP 2
UMAP 1
4
2
0
-2
-4
-6
-5.0
-2.5
0.0
2.5
5.0
pseudotime
12.5
10.0
7.5
5.0
2.5
0.0
1
2
3
4

FIG. S7

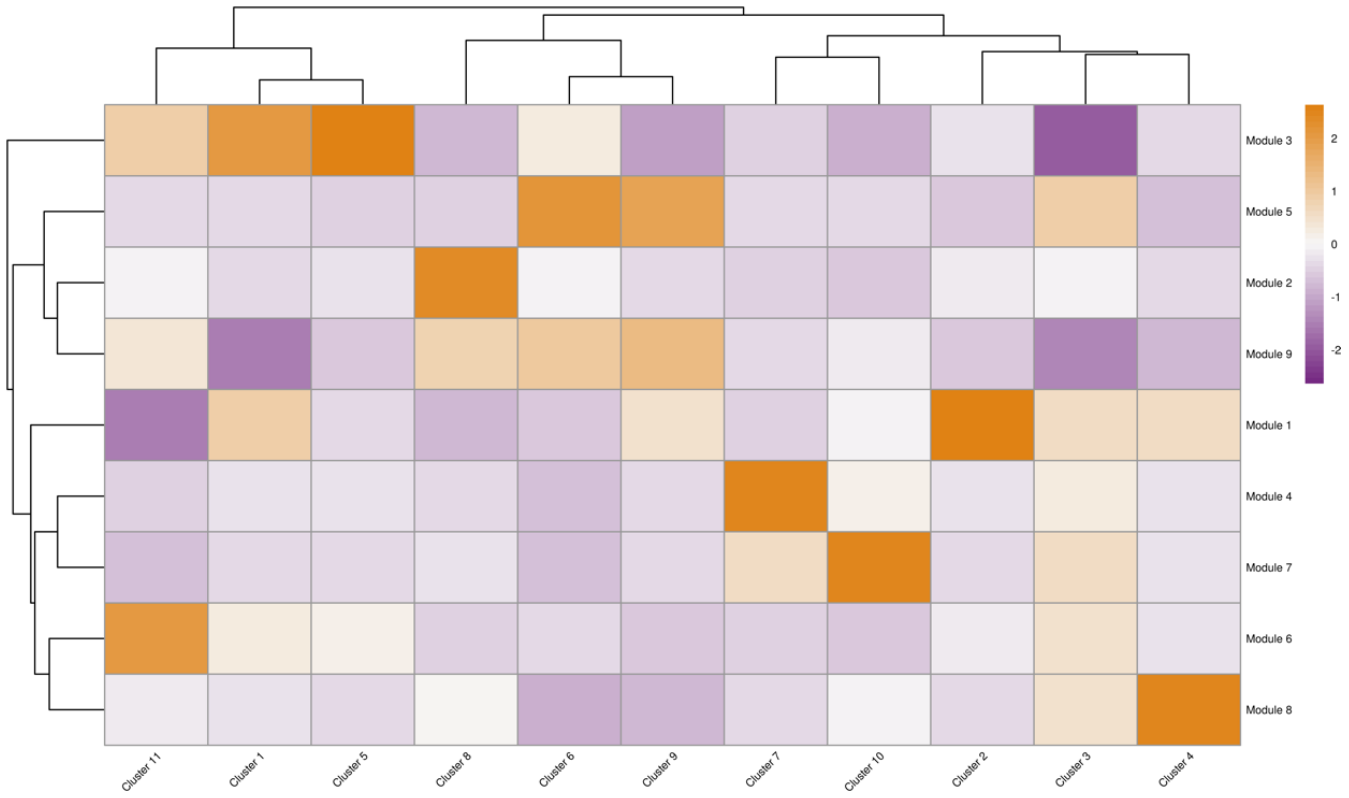
Module 3
Module 5
Module 2
Module 9
Module 1
Module 4
Module 7
Module 6
Module 8
2
1
0
-1
-2
Cluster 11
Cluster 1
Cluster 5
Cluster 8
Cluster 6
Cluster 9
Cluster 7
Cluster 10
Cluster 2
Cluster 3
Cluster 4

FIG. S8

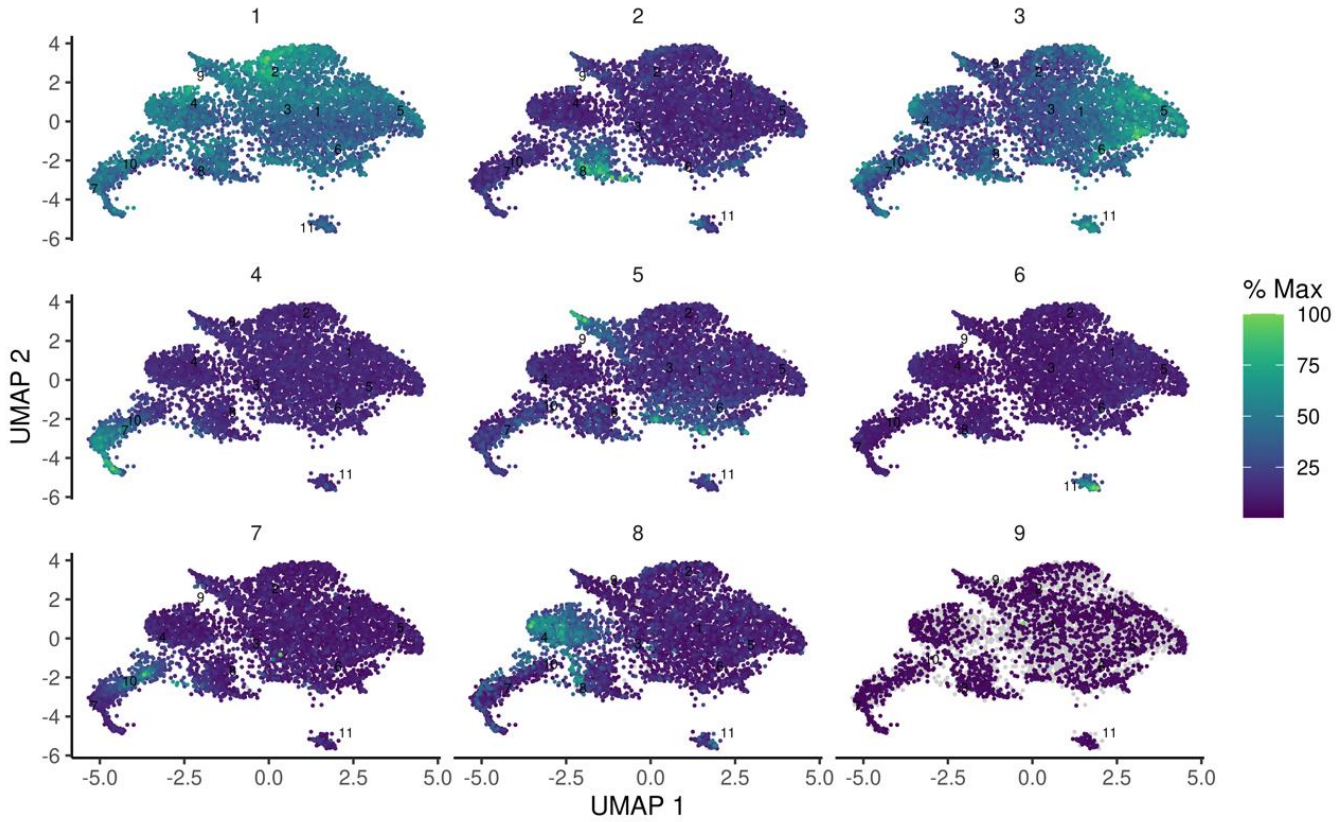

FIG. S9

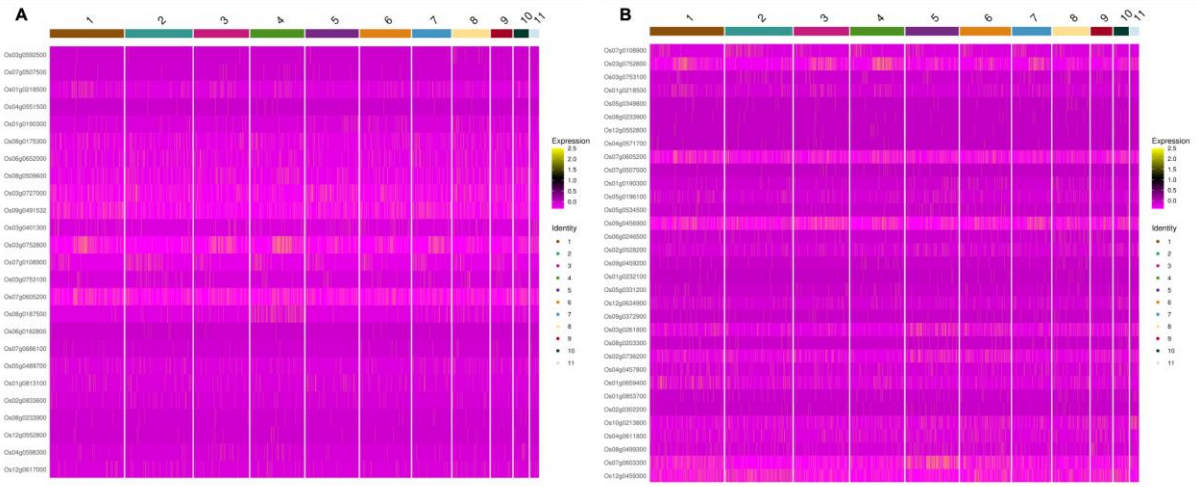

FIG. S10

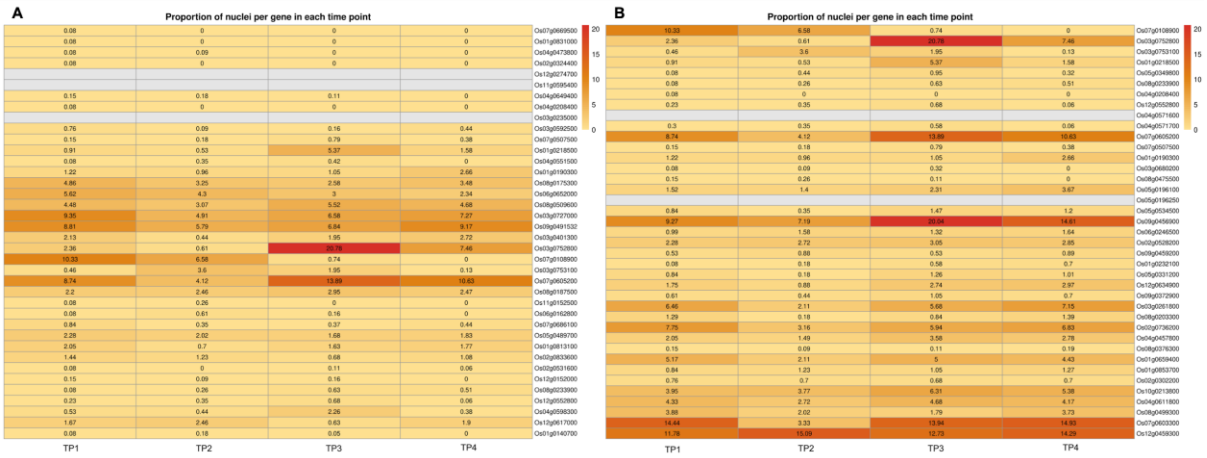
A
Proportion of nuclei per gene in each time point
TP1
TP2
TP3
TP4
B
Proportion of nuclei per gene in each time point
TP1
TP2
TP3
TP4

FIG. S11

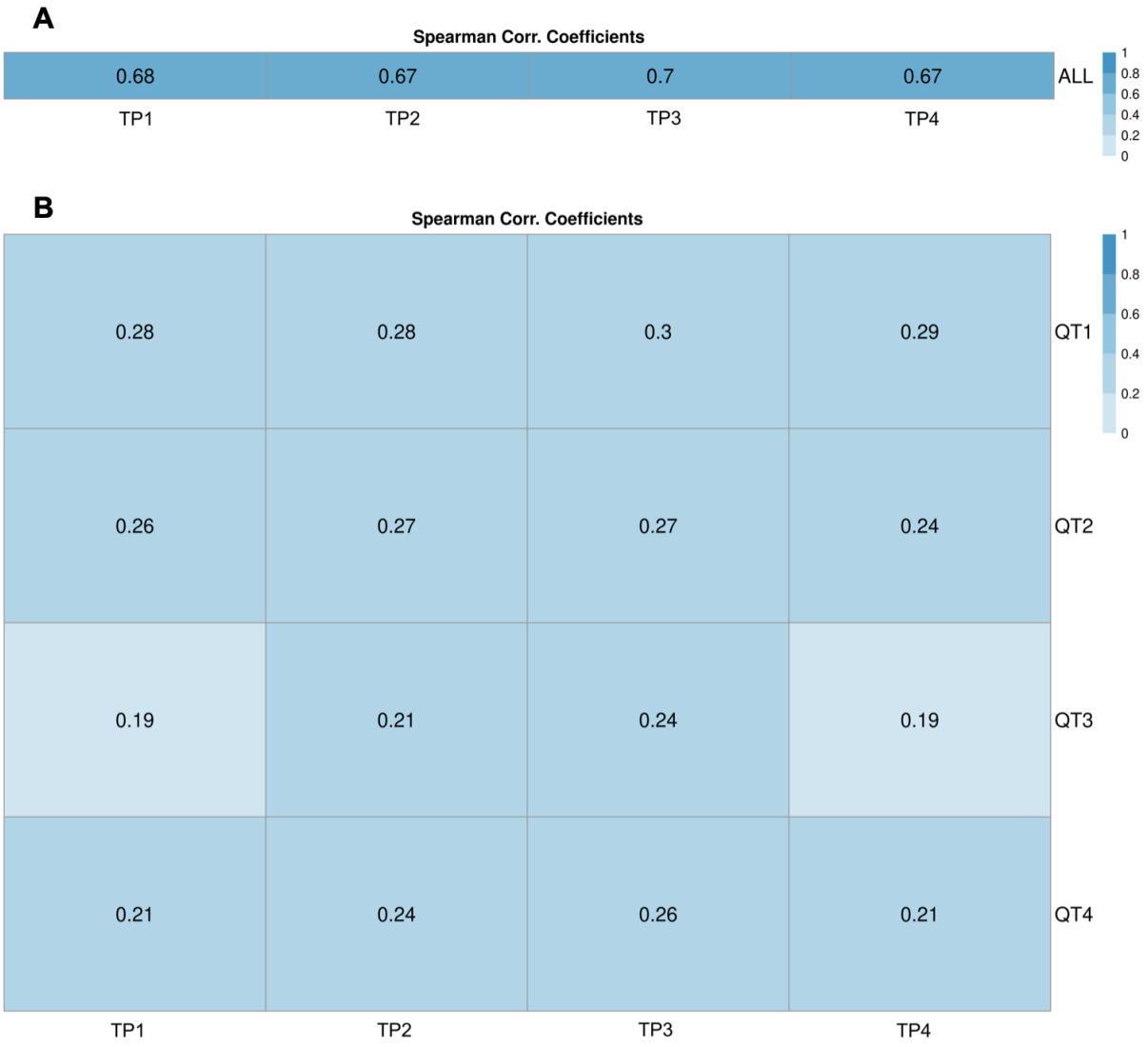
A
Spearman Corr. Coefficients
0.68
0.67
0.7
0.67
ALL
TP1
TP2
TP3
TP4
1
0.8
0.6
0.4
0.2
0
B
Spearman Corr. Coefficients
0.28
0.28
0.3
0.29
QT1
0.26
0.27
0.27
0.24
QT2
0.19
0.21
0.24
0.19
QT3
0.21
0.24
0.26
0.21
QT4
TP1
TP2
TP3
TP4
1
0.8
0.6
0.4
0.2
0

FIGURE S12

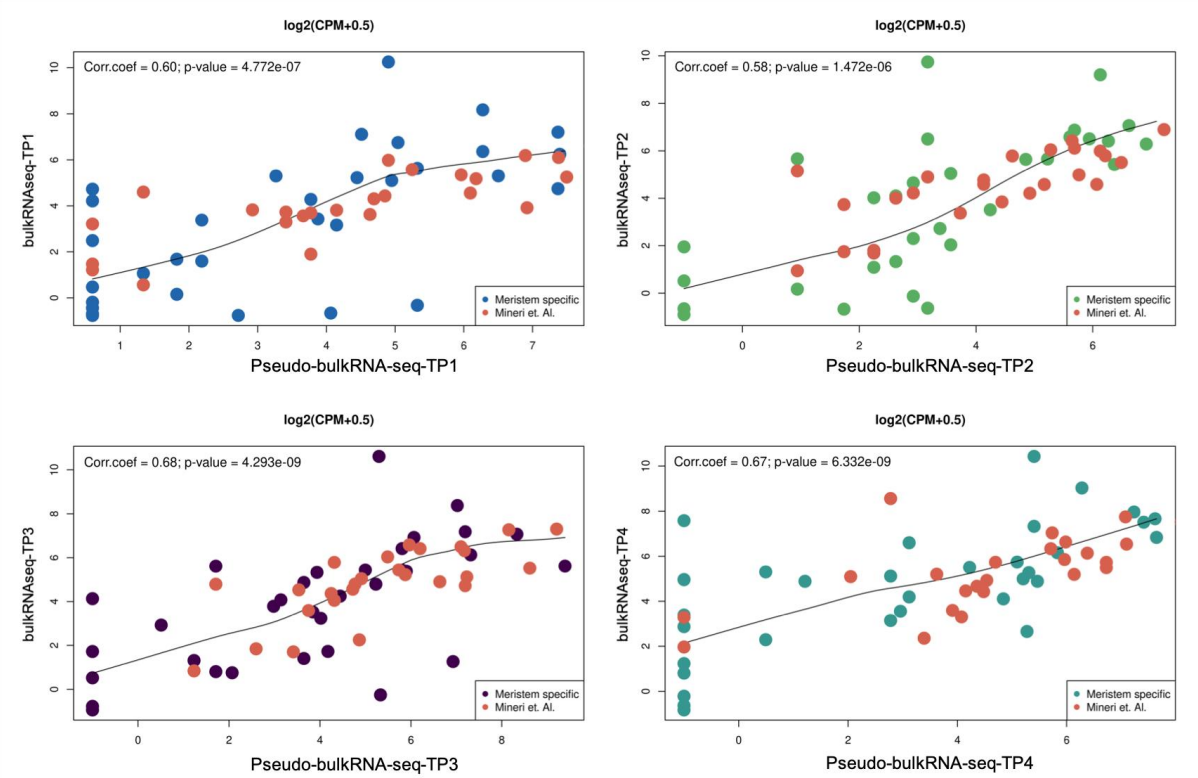
log2(CPM+0.5)
Corr.coef = 0.60; p-value = 4.772e-07
bulkRNAseq-TP1
Pseudo-bulkRNA-seq-TP1
Meristem specific
Mineri et. Al.
log2(CPM+0.5)
Corr.coef = 0.58; p-value = 1.472e-06
bulkRNAseq-TP2
Pseudo-bulkRNA-seq-TP2
Meristem specific
Mineri et. Al.
log2(CPM+0.5)
Corr.coef = 0.68; p-value = 4.293e-09
bulkRNAseq-TP3
Pseudo-bulkRNA-seq-TP3
Meristem specific
Mineri et. Al.
log2(CPM+0.5)
Corr.coef = 0.67; p-value = 6.332e-09
bulkRNAseq-TP4
Pseudo-bulkRNA-seq-TP4
Meristem specific
Mineri et. Al.

FIGURE S13

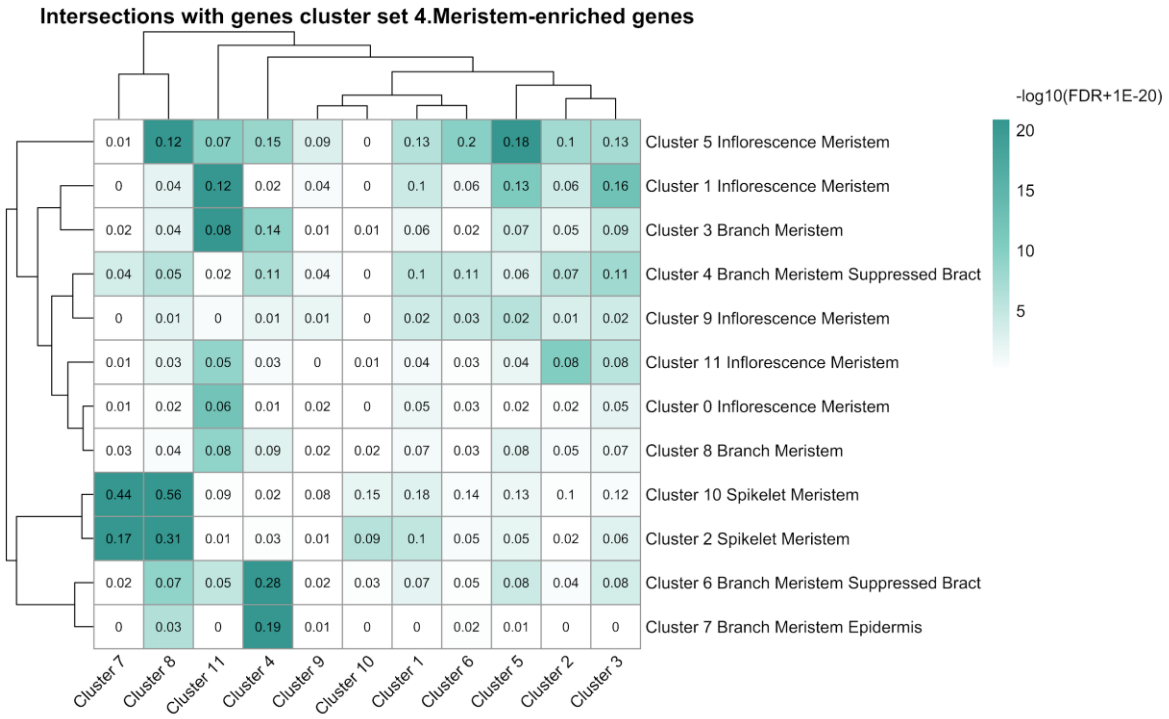
Intersections with genes cluster set 4.Meristem-enriched genes
-log10(FDR+1E-20)
20
15
10
5
Cluster 5 Inflorescence Meristem
Cluster 1 Inflorescence Meristem
Cluster 3 Branch Meristem
Cluster 4 Branch Meristem Suppressed Bract
Cluster 9 Inflorescence Meristem
Cluster 11 Inflorescence Meristem
Cluster 0 Inflorescence Meristem
Cluster 8 Branch Meristem
Cluster 10 Spikelet Meristem
Cluster 2 Spikelet Meristem
Cluster 6 Branch Meristem Suppressed Bract
Cluster 7 Branch Meristem Epidermis
Cluster 7
Cluster 8
Cluster 11
Cluster 4
Cluster 9
Cluster 10
Cluster 1
Cluster 6
Cluster 5
Cluster 2
Cluster 3

FIGURE S14

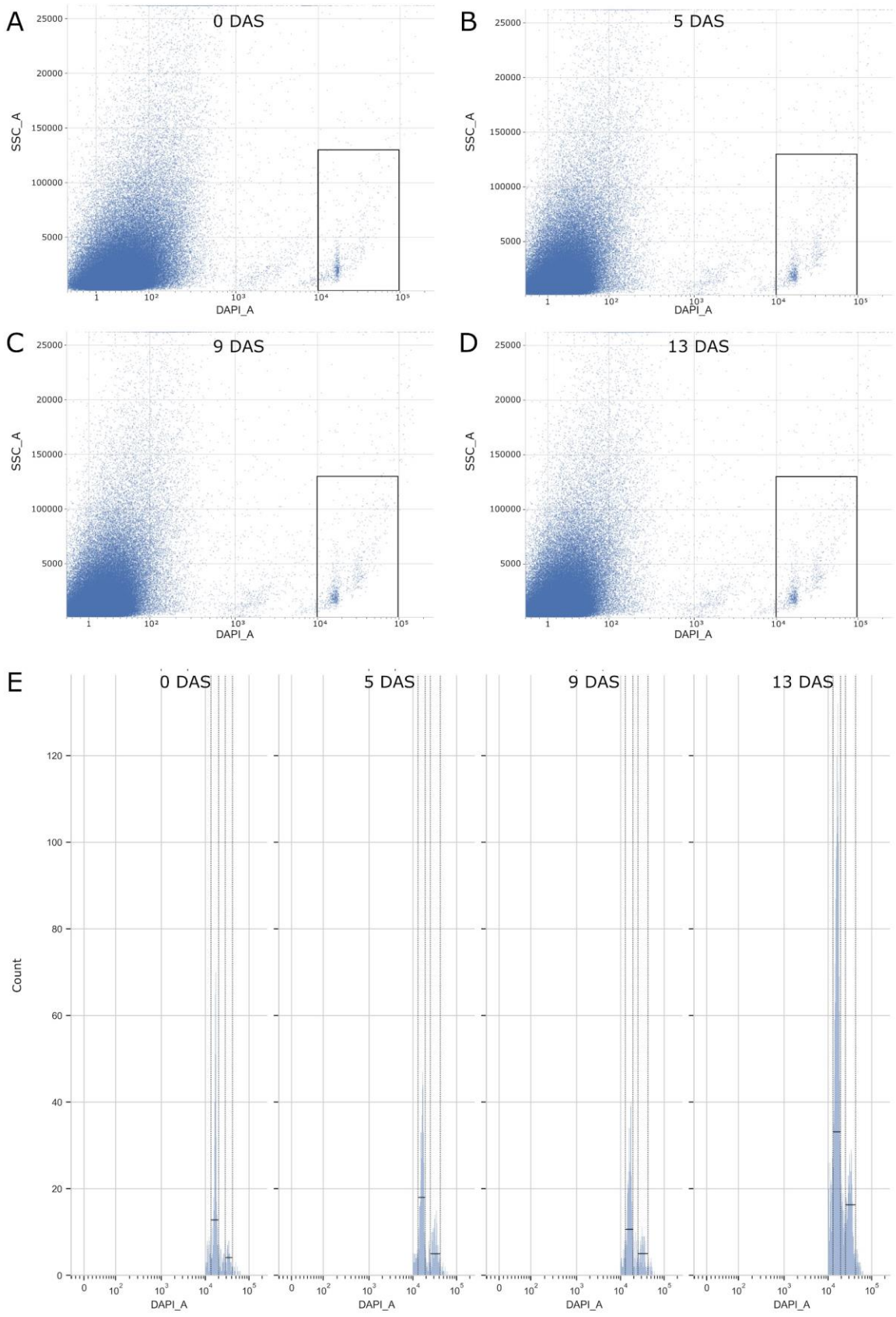

SUPPLEMENTARY FIGURES CAPTIONS

Fig. S1: Distribution of read counts per nuclei

Histogram reporting the distribution of the number of UMI counted per nuclei. The dotted red line at 200 indicates the threshold used for quality control and filtering.

Fig. S2: Distribution of the number of transcripts per nuclei

Histogram reporting the distribution of the number of transcripts expressed per nuclei. The dotted red line at 200 indicates the threshold used for quality control and filtering.

Fig. S3: UMAP of clusters.

UMAP of single nuclei clusters identified by Seurat. Color codes are used to indicate different clusters according to the legend.

Fig. S4: Proportion of nuclei within each cluster associated with each time point.

Barplot highlighting the number of nuclei assigned to each cluster at every time point. Time points are indicated according to the color code in the legend (TP1, TP2, TP3 and TP4) while clusters are visualized on the bottom of the bars. The number of nuclei per time point is reported on the top of each bar.

Fig. S5: Semantic clustering analysis:

A) Sankey diagram linking clusters (left portion of the plot) to semantic topics (right part of the plot). B) network of enriched molecular function GO terms; nodes are coloured according to the weight of enriched GO terms in the definition of the underlying semantic topic.

Fig. S6: Pseudo time trajectories across clusters: Pseudo time gene expression trajectories identified by Monocle 3.0. Brighter colors indicate later pseudo time progression. Starting point arbitrarily set at cluster 1 and 5.

Fig. S7: Association between clusters and modules.

Proportion of shared genes between clusters and modules. Proportions are reported in the form of standardized Z-scores. Clusters are reported on the rows, genes on the columns. Standardization is performed on the columns (clusters)

Fig. S8: Expression of module specific genes.

Modules are displayed in numerical order (1-9), top left to bottom right. For every module a UMAP is represented; for every cell the fraction (0-100%) of expressed module-specific genes is indicated according to the color gradient on the right.

Fig. S9: Expression of SAM/inflorescence identity genes across clusters

Expression of a selected list (Supplementary Table S5) of marker genes associated with SAM/inflorescence identity across each time point (TP1, TP2, TP3 and TP4). A) markers established by *in situ* hybridization/derived from the literature; B) genes differentially expressed and up-regulated according to Mineri et al 2023. Genes are reported on the rows and clusters on the columns. Expression levels are reported as the $\log_2$(FC) of the average expression of the gene in a cluster with respect to the average in all other cells.

Fig. S10: Proportion of nuclei expressing SAM/inflorescence identity genes in the four time points.

Proportion (%) of nuclei expressing selected marker genes (Supplementary Table S5) at each time point (TP1, TP2, TP3 and TP4). A) markers established by *in situ* hybridization/derived from the literature; B) genes differentially expressed and up-regulated according to Mineri et al 2023. Gene are indicated on the rows, time points on the columns, the % of cells expressing a gene is reported in every cell.

Fig. 11: Correlation of gene expression between pseudo-bulk snRNAseq and bulk RNAseq

A) Spearman correlation coefficients calculated on 23312 genes expressed by in datasets at any time point; B) Spearman correlation coefficients at different levels of expression: QT1: $\log_2$(CPM+1) < 2; QT2: 2 <= $\log_2$(CPM+1) <3.9; QT3: 3.9<= $\log_2$(CPM+1) <5.5; QT4: $\log_2$(CPM+1) >=5.5. Time points are indicated on the bottom of the plot.

Fig. S12: Scatterplots of gene expression profiles of selected genes between bulk-RNAseq and pseudo-bulk snRNA-seq

A) Time point 1; B) Time point 2; C) Time point 3; D) Time point 4. In all the plots gene expression levels estimated from the pseudo-bulk snRNA-seq are reported on the X axis, expression levels estimated from bulk-RNAseq on the Y axis. Correlation coefficients (Spearman correlation) and p-values for the statistical significance of the correlation are reported at the top.

Fig. S13: Intersection of cluster-specific genes with Zong et Al.

The Heatmap displays the proportion of cluster-specific genes identified by our analyses (rows), shared with meristem specific clusters as defined by Zong et al. 2022 (columns). The color intensity indicates the significance of the intersection expressed according to the hypergeometric distribution. P-values were corrected with the Benjamini-Hochberg correction for the control of the False Discovery Rate. A -log10() scaling was applied following FDR correction (see bar on the right).

Fig. S14: Fluorescence-activated sorting of nuclei.

Nuclei were sorted based on DAPI area (A-D) and DAPI mean fluorescence intensity (E). A-D: Biparametric-flow cytometric analyses of DAPI-stained nuclei (DAPI_A) for each experimental condition (A: 0 DAS; B: 5 DAS; C: 9 DAS; D: 13 DAS), examining blue fluorescence, detected using a 450-nm/40-nm band pass filter, versus side scatter (SSC_A, area filter). The gates (black rectangles) designate the region used as the sort window for nuclei isolation. E: Uniparametric display of the 450-nm fluorescence emission from DAPI stained nuclei for each sample (left to right: 0, 5, 9, and 13 DAS). Two sorting windows (vertical dotted gray lines) were used surrounding the two major peaks.